Frictional energy dissipation due to phonon resonance in two-layer graphene system

Zhiyong Wei (zywei@seu.edu.cn)
Southeast University https://orcid.org/0000-0001-8686-451X
Yi Tao
Southeastern University
Xi Lu
Southeast University
Yajing Kan
Southeast University
Yan Zhang
Southeast University
Yunfei Chen
Southeast University

Research Article

Keywords: phonon resonance, washboard frequency, energy dissipation, graphene

Posted Date: June 8th, 2022

DOI: https://doi.org/10.21203/rs.3.rs-1726359/v1

Frictional energy dissipation due to phonon resonance in two-layer graphene system

Zhiyong Wei*, Yi Tao, Xi Lu, Yajing Kan, Yan Zhang, and Yunfei Chen*

Jiangsu Key Laboratory for Design & Manufacture of Micro/Nano Biomedical Instruments and School of Mechanical Engineering, Southeast University, Nanjing 211189, People's Republic of China

Corresponding author

Email: zywei@seu.edu.cn (Z. W.); yunfeichen@seu.edu.cn (Y. C.)

Abstract

The frictional energy dissipation mechanism of a supported two-layer graphene film under the excitation of the model washboard frequency is investigated by molecular dynamics simulations. The results show that two local maxima in the energy dissipation rate occur at special frequencies as the excitation frequency increases from 0.1 to 0.6 THz. By extracting the vibrational density of states of the graphene, it is found that large numbers of phonons with frequencies equal to the excitation frequency are produced. A two-degree of freedom mass-spring model is proposed to explain the molecular dynamics results. Our study indicates that the phonons would resonate with the frictional excitation once the washboard frequency is close to the natural frequency of the frictional system, leading to remarkable local maxima in energy dissipation rate.

Keywords: phonon resonance, washboard frequency, energy dissipation, graphene

1. Introduction

Friction is a common phenomenon that occurs in aspects of our lives. Nevertheless, it is difficult to give a universal understanding of the energy dissipation mechanism due to its complexity. For example, the friction generally shows a gradually decreasing trend with the increase of sliding velocity on the macro-scale [1], while on the atomic scale the friction usually presents a trend of gradual increase with the increase in the sliding velocity [2-3]. The variation of friction is closely related to the energy dissipation mechanism in the friction process [4]. For a long time, the researchers generally use the potential barrier height [5-6] and shear strength [7-8] of friction interface to compare and quantify the magnitude of friction force when two interfaces slide relative to each other. The maximum friction generally implies a unique energy dissipation channel [9]. However, the fundamental physics involved in the friction process, such as the phonon [10-13] and/or electron [14-15] related dissipation, remains unclear.

The friction process can excite large numbers of non-equilibrium phonons (elastic waves) [16], which dissipates the mechanical kinetical energy through the phonon scattering [11, 17-18] with other phonons, boundaries and/or impurities. As for the two-wall carbon nanotube oscillators, Tangney et al [19] showed that the friction between the inter-tube and the out-tube would have a maximum value when the group velocity of excited phonons was equal to the sliding velocity. Panizon et al [20] deduced a formula to calculate the friction force based on linear response theory. Their results show that the resonance would occurs and can cause a local maximum in the friction force when the group velocity of the excited phonons is equal to the phase velocity. Our recent theoretical and experimental studies [21] also show that when the atomic force microscope (AFM) tip slides on the crystal surface, the phonon mode of the substrate excited by the slider also resonates with the entire friction system, resulting in multiple local maxima of friction force with the increase of sliding velocity. The similar

resonance principle is also adopted by quartz crystal microbalance (QCM) to measure the energy dissipation rate of adsorbed films [22] and two-dimensional materials [23]. Therefore, we speculated that the excited phonons will be strengthened and the energy dissipation will increase if the excited phonons in the friction process are consistent with the natural frequency of the whole friction system. Conversely, when the excited phonon frequency is far away from the natural frequency of the friction system, the energy dissipation may decrease or be suppressed.

In order to verify the above conjecture, this work investigated the frictional energy dissipation mechanism caused by inter-layer shear motion of graphene films by molecular dynamics (MD) method. An external periodic excitation is applied to make one layer of graphene vibrate tangentially on the other layer of graphene. The similar method is also used by Sokoloff to explore the possible nearly frictionless sliding for mesoscopic solids [24]. The frequency of the periodic excitation can be analogy for the washboard frequency v/a in the dry friction with sliding velocity v and substrate period a. The resultant energy dissipation due to periodic excitation is also extremely important for the performance of graphene-based MEMS devices [25-26]. Our study shows that two local maxima in the energy dissipation rate of the system does appear at special excitation frequencies. We further explain the simulation results in details by extracting the vibrational density of states and the natural frequency of the system with various system parameters.

2 Model and method

Figure 1(a) shows the atomic model for all our MD simulations, including a period-excited upper graphene and a supported lower graphene. The in-plane size is about 90 x 104 $Å^2$ and there are 6912 atoms in the simulation system. To illustrate the details of the model more clearly, a schematic diagram of the atomic model is also shown in Figure 1 (b). The upper graphene is connected to a support by three independent springs along x, y, and z direction with stiffness k_x, k_y and k_z, respectively. The k_x and k_y are the

shearing stiffness of the spring. By applying periodic excitation to the support end along the in-plane direction, like the washboard excitation in dry friction, the upper graphene would vibrate relative to the lower graphene and result in energy dissipation. To simplify the simulations, we also used a set of springs along x, y and z directions with stiffness of k_{subx}, k_{suby}, and k_{subz} to attach to the lower graphene, while the other ends of these springs are fixed. Both k_{subx} and k_{suby} are set as the effective interfacial shearing stiffness k_0 between two graphene layers at the state of equilibrium. The k_0 depends on the used interlayer interactions and can be calculated by differencing the interfacial shearing force with respect to the lateral displacement [21].

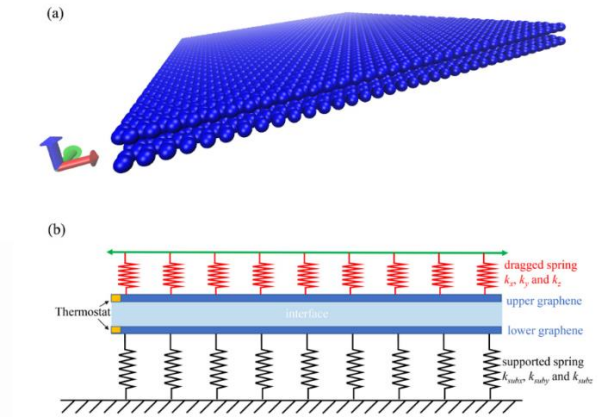

Figure 1. The atomic model (a) and the corresponding schematic diagram (b) to investigate the energy dissipation of two-layer graphene system under periodic excitations. The stiffness k_{subx}, k_{suby}, and k_{subz} of the supported springs are set as the effective interfacial stiffness of two-layer graphene, to simulate the lower graphene being supported on the bulk graphite. The stiffness k_x, k_y, and k_z of the dragged springs can be adjusted freely based on the effective interfacial stiffness of two-layer graphene in the molecular dynamics simulations.

In order to distinguish the excited phonons in the friction process from the intrinsic phonons within the graphene at the finite temperature, the simulation temperature is set at 0.001 K. The optimized Tersoff potential [27] is used to describe the carbon-carbon interactions within each graphene layers, while the Lennard-Jones (LJ) potential [28] for the interlayer carbon-carbon interactions between the two graphene layers. The shearing stiffness between the two-layer graphene is calculated to be k_0=7.47 eV/Å

from the used LJ potential. We first equilibrium the simulation system at 0.001 K for 500 ps, and then a periodic excitation with the frequency f_0 and the amplitude Am are applied to the support to imitate the dry friction on atomic smooth surface [21, 24]. The Langevin thermostats on both the upper and lower graphene are used to control the temperature of the simulation system. There are no fixed atoms in the simulation system. The periodic boundary conditions are applied along the in-plane directions. The equations of motions are solved with the velocity-Verlet algorithm with a timestep of 0.5 fs.

3. Results and discussion

Firstly, we set $k_x = k_y$ to k_0, and the amplitude and excitation frequency to Am= 0.1 Å and f_0=0.1 THz, respectively. Figure 2 shows the relation between the accumulated energy in the thermostat and the effective simulation time. The results show that the accumulative energy is proportional to the simulation time, indicating the energy dissipation is stable during the periodic excitation. When we increased the excitation frequency, such as to 0.2 THz, the cumulative energy in the thermostat still shows a good linear relation with the simulation time. Thus, the energy dissipation rate in the dissipative system under periodic excitation is defined as the proportional coefficient between the accumulated energy and the effective simulation time.

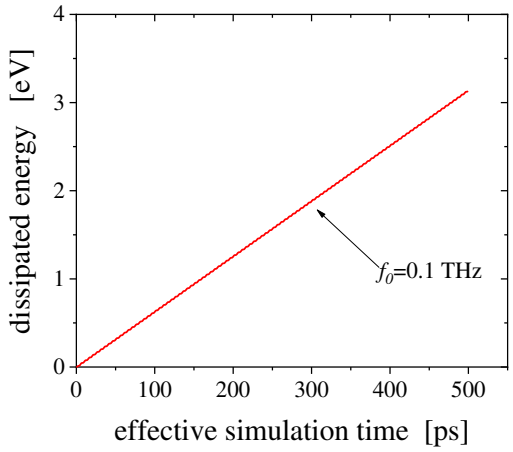

Figure 2. The dissipated energy in the thermostat as a function of the effective simulation time with the excitation frequency of f_0=0.1 THz. The energy dissipation rate is defined as the ratio of the dissipation energy to the effective simulation time.

Next, the excitation frequency is gradually increased from 0.1 to 0.6 THz in the MD simulation, and the corresponding energy dissipation rate is calculated as mentioned above. Figure 3(c) shows that there are two local maxima for the energy dissipation rate when the excitation frequency equals 0.21 or 0.36 THz. In order to confirm our observations, we reduced the shearing stiffness of the spring between the support and the upper graphene layer by 2 times and 4 times, respectively. In these cases, the interfacial shearing stiffness between the two graphene layers is greater than that of the spring between support and the upper graphene layer. Figure 3(a) and (b) show that two maxima in the energy dissipation rate still appears with the increase of excitation frequency from 0.1 to 0.6 THz. We also increase the shearing stiffness of the spring by a factor of 2, corresponding to the situation on which the interfacial shearing stiffness is less than that of the spring. Figure 3 (d) shows that the energy dissipation rate of the system only has a maximum value with the increasing excitation frequency. However, the energy dissipation rate with the excitation frequency in Fig. 3(d) can obviously be fitted using two Lorentz functions with center frequency of 0.25 and 0.40 THz, indicating these two special excitation frequencies can result in significant energy dissipation in the friction system. In addition, it is observed from Figure 3(a) to 3(d) that the excitation frequencies corresponding to the maximum value of energy dissipation rate gradually shift to high frequency region with the increasing shearing stiffness of the springs between the support and the upper graphene layer. For example, when the shearing stiffness increases from $0.25k_0$ to $2.0k_0$, the excitation frequency corresponding to the first peak of energy dissipation rate increases from 0.16 to 0.25 THz, and the excitation frequency corresponding to the second peak of the energy dissipation rate also increases from 0.34 to 0.40 THz.

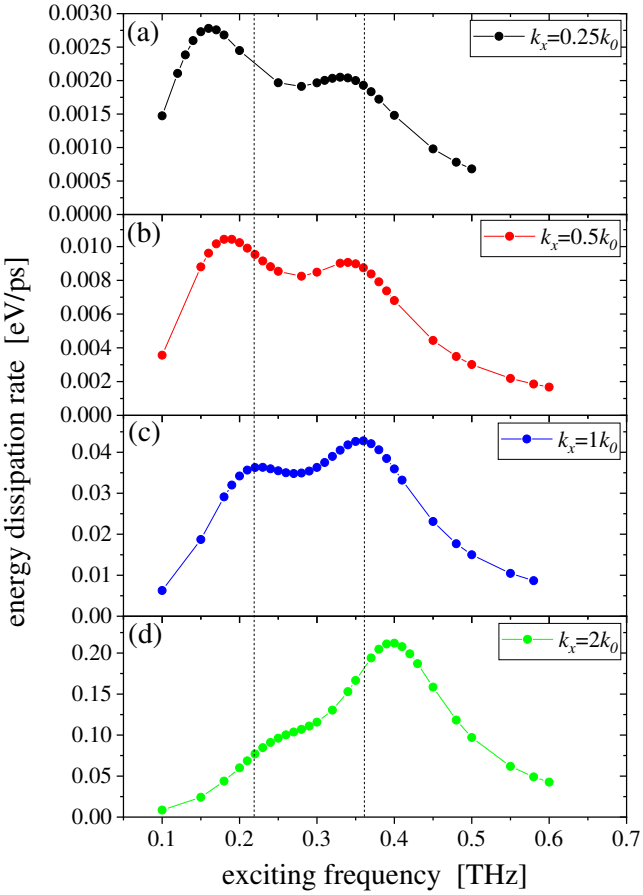

Figure 3. The energy dissipation rate as a function of the exciting frequency in the MD simulations with various shearing stiffness k_x of dragged spring: (a) k_x =0.25 k_0, (b) k_x =0.5 k_0, (c) k_x =1k_0, (d) k_x=2k_0, where k_0 is the shearing stiffness between two graphene layers under the state of equilibrium. The two vertical dashed lines are used to guide the shift of excitation frequency corresponding to the local maxima in the energy dissipation rate.

In order to understand the relationship between the energy dissipation rate and the excitation frequency, we performed the Fourier transform to the velocity autocorrelation function of the atoms in the lower graphene layer. Thus, the vibrational density of states (vDOS) [29] in the lower graphene can be obtained under periodic excitation. Figure 4 shows that when the excitation frequency is 0.1 THz, the phonons with frequencies around 0.1 THz are obviously present in the vDOS of the substate, while other phonon frequencies are strongly suppressed due to the low simulation temperature. When changing the excitation frequency, the excited phonons with the same frequency appear in the vDOS of the lower graphene layer. This indicates that

large numbers of phonons with the same frequency as the excitation frequency are generated in the lower graphene under external periodic excitation. It is expected that the local maximum of the energy dissipation rate maybe results from the phonon resonance when the excited phonons in the substrate have the same frequency with the natural frequency of the friction system.

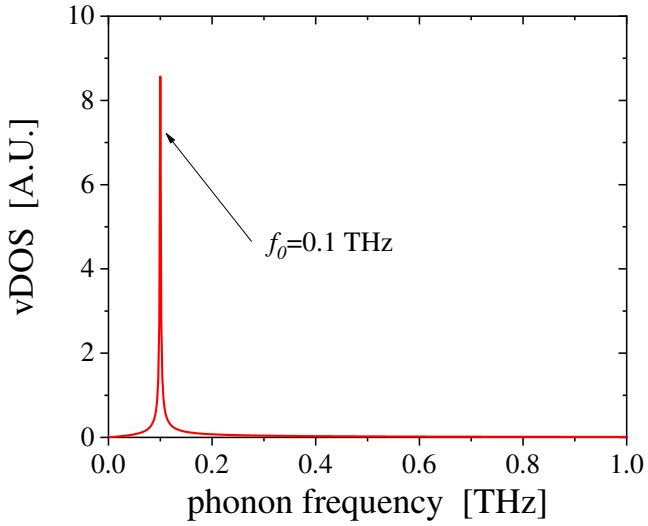

Figure 4. The vibrational density of states of the lower graphene layer with the excitation frequency of f_0=0.1 THz. The high-frequency phonons are suppressed and not shown here due to the low simulation temperature.

In order to confirm the above statement, a two-degree of freedom mass-spring model is established as shown in the inset of Fig. 5. By comparing with the MD model, we set both mass m_1 *and* m_2 in the model as $m_1=m_2=m=N \times m_c$, where N is the atom number within the upper graphene layer and m_c is the mass of each carbon atom. There is no normal load applied in the MD simulation and the energy dissipation mainly depends on the shearing stiffness between the support and the upper graphene layer. Thus, the spring stiffness k_{in} that connects the two mass is set as the effective interfacial shearing stiffness k_0 between the two graphene layers in the state of equilibrium, i.e. $k_{in}=k_0$. The spring stiffness k_{sub} that connects the lower mass and the fixed substrate is also set as k_0, i.e. $k_{sub}=k_0$, and the spring stiffness k that connects the upper mass and the vibrating support can be adjusted with the MD model. When a small periodic excitation

$$y_0 = A \times \cos(\omega t) \tag{1}$$

is applied on the vibration end, the resultant equations of motion for the two-degree of freedom model can be written as

$$\begin{cases} m\ddot{y}_1(t) + m\dot{y}_1(t)\gamma_1 = -y_1(t)\cdot k_{sub} - (y_1(t) - y_2(t))\cdot k_{in} \\ m\ddot{y}_2(t) + m\dot{y}_2(t)\gamma_2 = -(y_2(t) - y_1(t))\cdot k_{in} - (y_2(t) - y_0(t))\cdot k \end{cases}, \tag{2}$$

where A is a small amplitude, $\omega=2\pi f_0$ is the excitation angular frequency, y_1 and y_2 are the corresponding displacement of the lower and the upper degree of freedom, γ_1 and γ_2 are their corresponding damping. By solving the above equation, it is found that the below condition should be satisfied when the amplitude of both degrees of freedom reach the maximum,

$$(k_{in} + k_{sub} - m\omega^2)(k_{in} + k - m\omega^2) = k_{in}^2 . \tag{3}$$

The detailed process to obtain the above equation can be found in the supporting information. As stated above, the interfacial shearing stiffness between the two graphene layers is equal to the shearing stiffness of the spring that connects the lower graphene layer and the fixed end in the MD simulations. This means that both k_{in} and k_{sub} should be constants and equal to k_0 in the two-degree of freedom mass-spring model, i.e. $k_{in}=k_{sub}=k_0$ to make the model be consistent with the MD simulations. So, we set $k_{sub}/k = k_{in}/k = k_0/k = 1/\alpha$, then the predicted excitation angular frequency that responds to the maximum energy dissipation rate in the friction system should be the two solutions to the Eq. (3), i.e. ω_- and ω_+, which can be easily obtained. The two special frequencies ω_- and ω_+ are the natural angular frequency of the two degrees of freedom, which are shown in Figure 5 as a function of the shearing stiffness of the spring $k=\alpha k_0$. It is shown that the two natural frequencies gradually increase when increasing the shearing stiffness of the dragged spring.

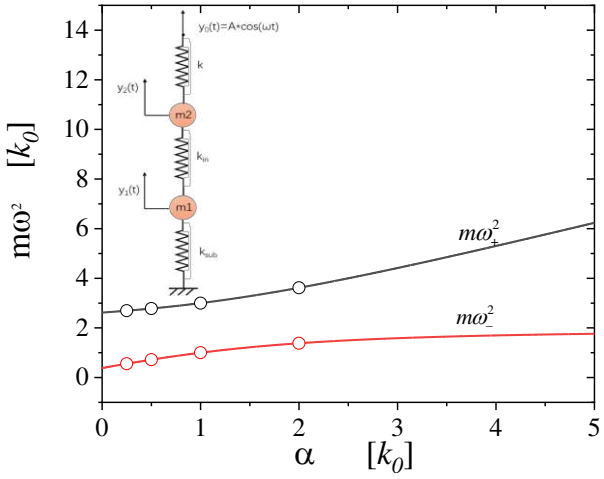

Figure 5. The natural frequencies of the two-degree of freedom mass-spring system as a function of the spring stiffness $k=\alpha k_0$. The circles on the lines represent four sets of simulation conditions in the MD. The inset is the two-degree of freedom mass-spring model to explain the MD simulations.

The special frequencies predicted by the two-degree of freedom mass-spring model are further compared with the results of MD simulation. Table 1 shows that, when the controlled shearing stiffness in MD simulations gradually changes from $0.25k_0$ to $2k_0$, the excitation frequency corresponding to the maximum energy dissipation rate of the system in Figure 3 is basically consistent with the natural frequency of the system predicted by the two-degree of freedom mass-spring model, which explains our MD simulation results.

Table 1. Comparison of the excitation frequencies that correspond to the local maxima in the energy dissipation rate of the two-layer graphene system between the MD simulations and mass-spring model.

k (k_0)	MD results (THz)		Predicted values from model (THz)	
	$\omega_-/(2\pi)$	$\omega_+/(2\pi)$	$\omega_-/(2\pi)$	$\omega_+/(2\pi)$
0.25	0.16	0.34	0.1567	0.3446
0.5	0.18	0.35	0.1781	0.3502
1	0.22	0.36	0.2100	0.3637
2	0.25	0.4	0.2469	0.3994

4.Conclusions

In summary, we investigated the frictional energy dissipation in two-layer graphene system under periodic excitation using molecular dynamics simulations. The results show that the energy dissipation rate present two local maxima when the excitation frequency increases gradually from 0.1 to 0.6 THz. By extracting the vibrational density of states, it is found that the periodic excitation can induce large numbers of phonons in the substrate, which has the same frequency with the excitation frequency. When the frequency of these phonons is equal to the natural frequency of the frictional system, the maximum in the energy dissipation rate appears. The proposed two-degree of freedom mass-spring model is also confirmed the MD results. This indicates that the energy dissipation rate in the frictional system can be modulated by controlling the washboard frequency and the resonant frequency of the system. This may explain the local maximum of the friction force with the sliding velocity [21]. It can also explain the commensurate interface has a larger friction force than the incommensurate interface because the excited phonon frequencies on both sides are always the same for the former while not for the later [30]. Our study establishes the relationship between the excitation frequency and energy dissipation rate in a model two-layer graphene system. The uncovered phonon resonance mechanism can be used to regulate the friction force and energy dissipation in many systems, including the nano-sensors, actuators etc.

Acknowledgments

The authors acknowledge the financial support from the National Natural Science Foundation of China (NO.52175161, NO. 51605090, NO.51575104), and the Southeast University “Zhongying Young Scholars” Project.

Data Availability

All data, models, or code generated or used during the study are available from the

corresponding author by reasonable request.

Supporting information

A. Solving the two-degree of freedom mass-spring model

In order to solve Eq. (2), the special solution y_1^* and y_2^* to Eq. (2) can be assumed as

$$\begin{cases} y_1^* = A_1 \cdot \cos(\omega t) + B_1 \cdot \sin(\omega t) \\ y_2^* = A_2 \cdot \cos(\omega t) + B_2 \cdot \sin(\omega t) \end{cases}, \tag{S1}$$

where A_1, B_1, A_2, and B_2 are the amplitude of the degrees of the freedom in the mass-spring model and to be determined by the external excitation. Thus, the energy dissipation rate P can be calculated as

$$\begin{aligned} P &= P_1 + P_2 = \frac{\omega}{2\pi}\left(\int_0^{2\pi/\omega} m\dot{y}_1^* \gamma_1 \dot{y}_1^* dt + \int_0^{2\pi/\omega} m\dot{y}_2^* \gamma_2 \dot{y}_2^* dt \right) \\ &= \frac{m\omega^2\gamma_1(A_1^2 + B_1^2) + m\omega^2\gamma_2(A_2^2 + B_2^2)}{2} \end{aligned} \tag{S2}$$

It is found from Eq. (S2) that the energy dissipation rate only depends on the amplitude of the two degrees of freedom. Inserting Eq. (S1) into Eq. (2), then we can obtain

$$\begin{cases} \{-A_1 m\omega^2 + B_1 m\omega\gamma_1 + A_1 k_{sub} + A_1 k_{in} - A_2 k_{in}\} \times \cos(\omega t) + \\ \{-B_1 m\omega^2 + A_1 m\omega\gamma_1 + B_1 k_{sub} + B_1 k_{in} - B_2 k_{in}\} \times \sin(\omega t) = 0 \\ \{-A_2 m\omega^2 + B_2 m\omega\gamma_2 - A_1 k_{in} + A_2 k_{in} + A_2 k - Ak\} \times \cos(\omega t) + \\ \{-B_2 m\omega^2 - A_2 m\omega\gamma_2 - B_1 k_{in} + B_2 k_{in} + B_2 k\} \times \sin(\omega t) = 0 \end{cases}. \tag{S3}$$

In order to make the above equation always be true, the below matrix should be satisfied as

$$\begin{bmatrix} k_{in} + k_{sub} - m\omega^2 & m\omega\gamma_1 & -k_{in} & 0 \\ -m\omega\gamma_1 & k_{in} + k_{sub} - m\omega^2 & 0 & -k_{in} \\ -k_{in} & 0 & k_{in} + k - m\omega^2 & m\omega\gamma_2 \\ 0 & -k_{in} & -m\omega\gamma_2 & k_{in} + k - m\omega^2 \end{bmatrix} \begin{bmatrix} A_1 \\ B_1 \\ A_2 \\ B_2 \end{bmatrix} = \begin{bmatrix} 0 \\ 0 \\ A \cdot k \\ 0 \end{bmatrix}, \tag{S4}$$

and A_1, B_1, A_2, and B_2 can be solved as

$$\begin{cases} A_1 = \dfrac{-A\omega_0^2\omega_{in}^2(\omega_{in}^4 - a \cdot b) - A\omega_0^2\omega_{in}^2\omega^2\gamma_1\gamma_2}{M} \\ B_1 = \dfrac{A\omega_0^2\omega_{in}^2(\omega\gamma_2 \cdot a + \omega\gamma_1 \cdot b)}{M} \\ A_2 = \dfrac{A\omega_0^2 \cdot a(a \cdot b - \omega_{in}^4) + A\omega_0^2\omega^2\gamma_1^2 \cdot b}{M} \\ B_2 = \dfrac{A\omega_0^2(\omega\gamma_2 \cdot a^2 + \omega^3\gamma_1^2\gamma_2 + \omega_{in}^4\omega\gamma_1)}{M} \end{cases}, \tag{S5}$$

where

$$\begin{cases} a = (\omega_{in}^2 + \omega_{sub}^2 - \omega^2) = (k_{in} + k_{sub} - m\omega^2)/m \\ b = (\omega_{in}^2 + \omega_0^2 - \omega^2) = (k_{in} + k - m\omega^2)/m \\ \mathrm{M} = (a \cdot b - \omega_{in}^4)^2 + \omega^2\gamma_2^2 \cdot a^2 + \omega^2\gamma_1^2 \cdot b^2 + \omega^4\gamma_1^2\gamma_2^2 + 2\omega_{in}^4\omega^2\gamma_1\gamma_2 \end{cases}, \quad \text{(S6)}$$

From Eq. (S6), the maximum amplitude and thus the maximum energy dissipation rate can be obtained only if the below equation is satisfied as

$$a \cdot b = \omega_{in}^4 . \quad \text{(S7)}$$

Eq. (S7) is completely equivalent to Eq. (3).

References

1. Baumberger, T.; Berthoud, P.; Caroli, C., Physical Analysis of the State- and Rate-Dependent Friction Law. Ii. Dynamic Friction. *Physical Review B* **1999**, *60*, 3928-3939.
2. Dong, Y.; Vadakkepatt, A.; Martini, A., Analytical Models for Atomic Friction. *Tribology Letters* **2011**, *44*, 367-386.
3. Gnecco, E.; Bennewitz, R.; Gyalog, T.; Loppacher, C.; Bammerlin, M.; Meyer, E.; Guntherodt, H. J., Velocity Dependence of Atomic Friction. *Phys. Rev. Lett.* **2000**, *84*, 1172-1175.
4. Granato, E.; Ying, S. C., Non-Monotonic Velocity Dependence of Atomic Friction. *Tribology Letters* **2010**, *39*, 229-233.
5. Dienwiebel, M.; Verhoeven, G. S.; Pradeep, N.; Frenken, J. W. M.; Heimberg, J. A.; Zandbergen, H. W., Superlubricity of Graphite. *Phys. Rev. Lett.* **2004**, *92*, 126101.
6. Vazirisereshk, M. R.; Hasz, K.; Carpick, R. W.; Martini, A., Friction Anisotropy of Mos2: Effect of Tip-Sample Contact Quality. *The journal of physical chemistry letters* **2020**, *11*, 6900-6906.
7. Zilibotti, G.; Righi, M. C., Ab Initio Calculation of the Adhesion and Ideal Shear Strength of Planar Diamond Interfaces with Different Atomic Structure and Hydrogen Coverage. *Langmuir* **2011**, *27*, 6862-6867.
8. Ma, T.-B.; Hu, Y.-Z.; Wang, H., Molecular Dynamics Simulation of Shear-Induced Graphitization of Amorphous Carbon Films. *Carbon* **2009**, *47*, 1953-1957.
9. Israelachvili, J. N., *Intermolecular and Surface Force*; Academic Press, 2011.
10. Lewis, S. P.; Pykhtin, M. V.; Mele, E. J.; Rappe, A. M., Continuum Elastic Theory of Adsorbate Vibrational Relaxation. *Journal of Chemical Physics* **1998**, *108*, 1157-1161.
11. Persson, B. N. J.; Ryberg, R., Brownian-Motion and Vibrational Phase Relaxation at Surfaces-Co on Ni(111). *Physical Review B* **1985**, *32*, 3586-3596.
12. Cannara, R. J.; Brukman, M. J.; Cimatu, K.; Sumant, A. V.; Baldelli, S.; Carpick, R. W., Nanoscale Friction Varied by Isotopic Shifting of Surface Vibrational Frequencies. *Science* **2007**, *318*, 780-783.
13. Daly, C.; Krim, J., Sliding Friction of Solid Xenon Monolayers and Bilayers on Ag(111). *Phys.rev.lett* **1996**, *76*, 803.
14. Kisiel, M.; Gnecco, E.; Gysin, U.; Marot, L.; Rast, S.; Meyer, E., Suppression of Electronic Friction on Nb Films in the Superconducting State. *Nature Materials* **2011**, *10*, 119-22.
15. Bruch, L. W., Ohmic Damping of Center-of-Mass Oscillations of a Molecular Monolayer. *Physical Review B* **2000**, *61*, 16201-16206.
16. Hu, R.; Krylov, S. Y.; Frenken, J. W. M., On the Origin of Frictional Energy Dissipation. *Tribology Letters* **2019**, *68*, 8.
17. Wei, Z.; Duan, Z.; Kan, Y.; Zhang, Y.; Chen, Y., Phonon Energy Dissipation in Friction between Graphene/Graphene Interface. *Journal of Applied Physics* **2020**, *127*, 015105.
18. Cammarata, A.; Nicolini, P.; Simonovic, K.; Ukraintsev, E.; Polcar, T., Atomic-Scale Design of Friction and Energy Dissipation. *Physical Review B* **2019**, *99*, 094303.
19. Tangney, P.; Louie, S. G.; Cohen, M. L., Dynamic Sliding Friction between Concentric Carbon Nanotubes. *Physical Review Letters* **2004**, *93*.
20. Panizon, E.; Santoro, G. E.; Tosatti, E.; Riva, G.; Manini, N., Analytic Understanding and Control of Dynamical Friction. *Physical Review B* **2018**, *97*.
21. Duan, Z., et al., Resonance in Atomic-Scale Sliding Friction. *Nano letters* **2021**, *21*, 4615-4621.
22. Krim, J.; H., S. D.; Chiarello, R., Nanotribology of a Kr Monolayer-a Quartz-Crystal

Microbalance Study of Atomic-Scale Friction. *Phys. Rev. Lett.* **1991**, *66*, 181-184.
23. Wada, N.; Ishikawa, M.; Shiga, T.; Shiomi, J.; Suzuki, M.; Miura, K., Superlubrication by Phonon Confinement. *Physical Review B* **2018**, *97*, 161403(R).
24. Sokoloff, J. B., Possible Nearly Frictionless Sliding for Mesoscopic Solids. *Physical Review Letters* **1993**, *71*, 3450-3453.
25. Takamura, M.; Okamoto, H.; Furukawa, K.; Yamaguchi, H.; Hibino, H., Energy Dissipation in Edged and Edgeless Graphene Mechanical Resonators. *Journal of Applied Physics* **2014**, *116*.
26. Luo, G.; Zhang, Z.-Z.; Deng, G.-W.; Li, H.-O.; Cao, G.; Xiao, M.; Guo, G.-C.; Tian, L.; Guo, G.-P., Strong Indirect Coupling between Graphene-Based Mechanical Resonators Via a Phonon Cavity (Vol 9, 383, 2018). *Nature Communications* **2019**, *10*.
27. Lindsay, L.; Broido, D. A., Optimized Tersoff and Brenner Empirical Potential Parameters for Lattice Dynamics and Phonon Thermal Transport in Carbon Nanotubes and Graphene. *Physical Review B* **2010**, *81*, 205441.
28. Wei, Z.; Yang, J.; Chen, W.; Bi, K.; Li, D.; Chen, Y., Phonon Mean Free Path of Graphite Along the C-Axis. *Applied Physics Letters* **2014**, *104*, 081903.
29. Sokhan, V. P.; Nicholson, D.; Quirke, N., Phonon Spectra in Model Carbon Nanotubes. *Journal of Chemical Physics* **2000**, *113*, 2007-2015.
30. Dong, Y., et al., Phononic Origin of Structural Lubrication. *Accepted in Friction, doi: 10.1007/s40544-022-0636-3* **2022**.

Statements and Declarations

All authors declare that No conflict of interest exists.

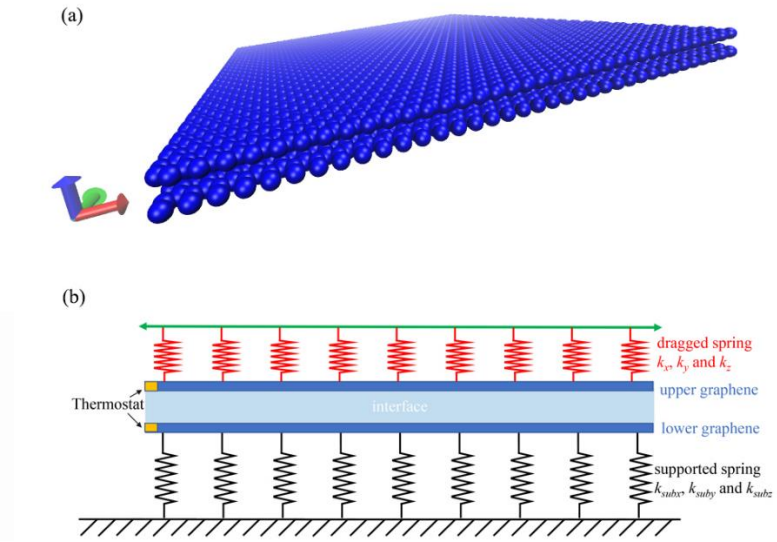

Figure 1. The atomic model (a) and the corresponding schematic diagram (b) to investigate the energy dissipation of two-layer graphene system under periodic excitations. The stiffness k_{subx}, k_{suby}, and k_{subz} of the supported springs are set as the effective interfacial stiffness of two-layer graphene, to simulate the lower graphene being supported on the bulk graphite. The stiffness k_x, k_y, and k_z of the dragged springs can be adjusted freely based on the effective interfacial stiffness of two-layer graphene in the molecular dynamics simulations.

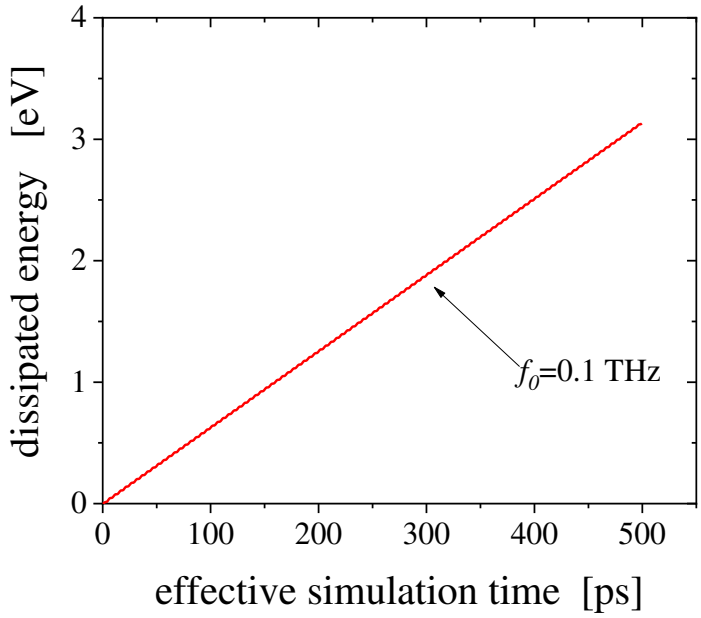

Figure 2. The dissipated energy in the thermostat as a function of the effective simulation time with the excitation frequency of f_0=0.1 THz. The energy dissipation rate is defined as the ratio of the dissipation energy to the effective simulation time.

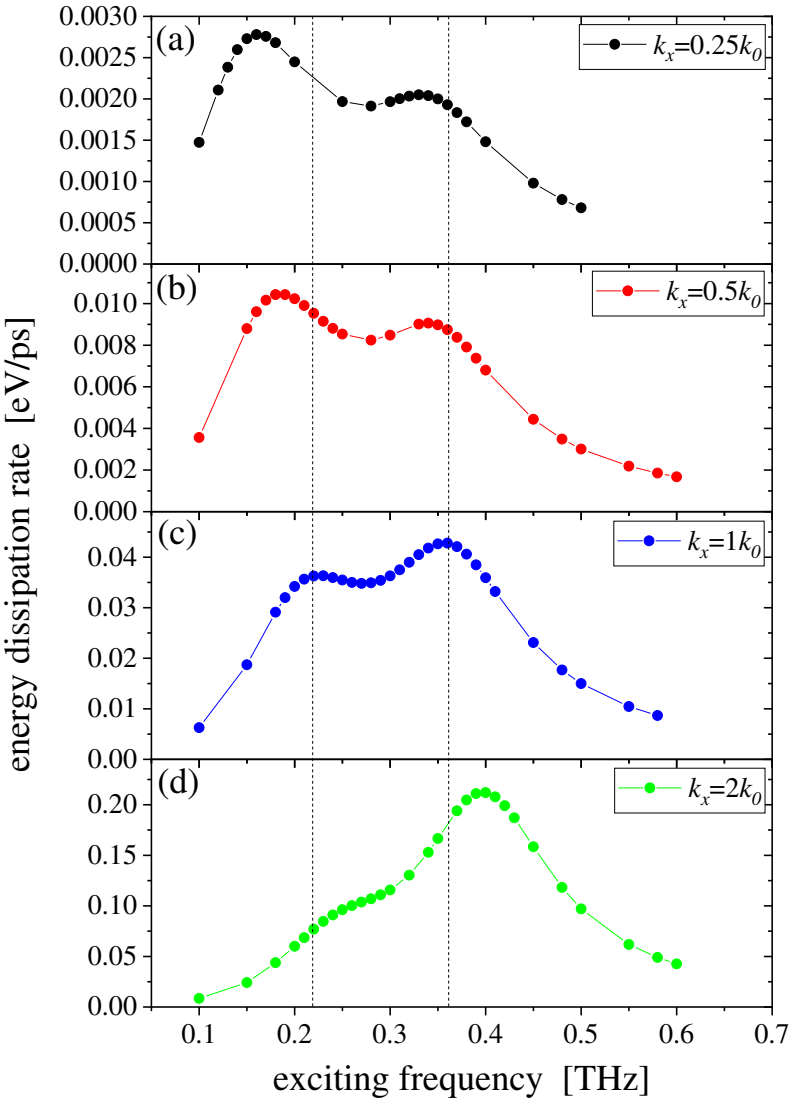

Figure 3. The energy dissipation rate as a function of the exciting frequency in the MD simulations with various shearing stiffness k_x of dragged spring: (a) k_x =0.25 k_0, (b) k_x =0.5 k_0, (c) k_x =1k_0, (d) k_x=2k_0, where k_0 is the shearing stiffness between two graphene layers under the state of equilibrium. The two vertical dashed lines are used to guide the shift of excitation frequency corresponding to the local maxima in the energy dissipation rate.

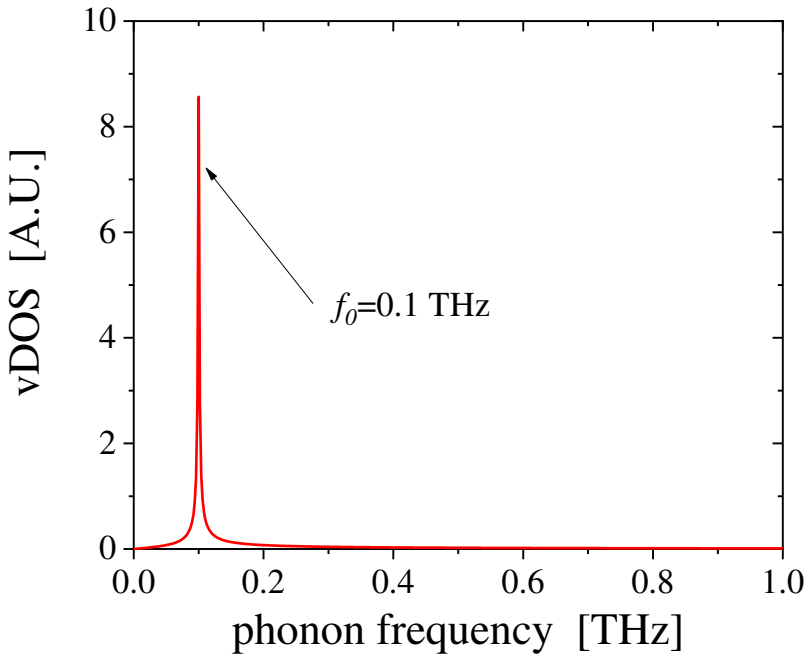

Figure 4. The vibrational density of states of the lower graphene layer with the excitation frequency of f_0=0.1 THz. The high-frequency phonons are suppressed and not shown here due to the low simulation temperature.

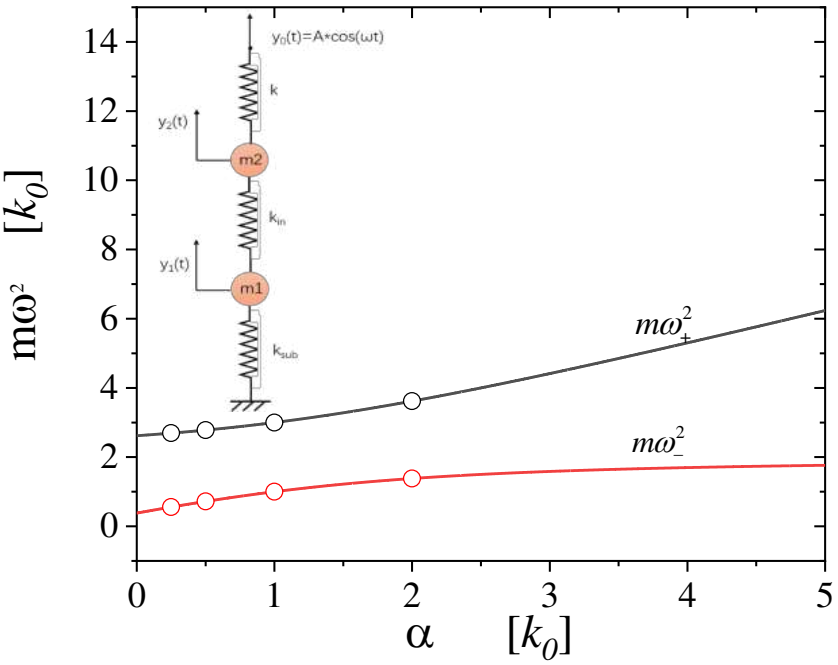

Figure 5. The natural frequencies of the two-degree of freedom mass-spring system as a function of the spring stiffness $k=\alpha k_0$. The circles on the lines represent four sets of simulation conditions in the MD. The inset is the two-degree of freedom mass-spring model to explain the MD simulations.

Table 1. Comparison of the excitation frequencies that correspond to the local maxima in the energy dissipation rate of the two-layer graphene system between the MD simulations and mass-spring model.

k (k_0)	**MD results (THz)**		**Predicted values from model (THz)**	
	$\omega_-/(2\pi)$	$\omega_+/(2\pi)$	$\omega_-/(2\pi)$	$\omega_+/(2\pi)$
0.25	0.16	0.34	0.1567	0.3446
0.5	0.18	0.35	0.1781	0.3502
1	0.22	0.36	0.2100	0.3637
2	0.25	0.4	0.2469	0.3994